www.cadanda.com
Computer-Aided Design AND APPLICATIONS™

Topological Modifications through Boolean Compositions on Algebraic Level Sets Constructed from B-rep Models

Pavan Kumar Vaitheeswaran[1] and Ganesh Subbarayan[2]

[1]Purdue University, pvaithee@purdue.edu
[2]Purdue University, ganeshs@purdue.edu

Corresponding author: Ganesh Subbarayan, ganeshs@purdue.edu

Abstract. Topological changes are common in problems where interfaces evolve with time, such as solidification, void nucleation or shape optimisation. If the evolving boundaries are represented explicitly, then modeling topological changes such as due to coalescence of two phases requires detection of collision between the two phases as well as computing the intersections of their boundaries. These are challenging operations for arbitrarily shaped interfaces. Thus, implicit representations of the boundary provided by the phase field or level set methods are often used to accommodate large topological changes. Such implicit representations also implicitize physically relevant geometrical parameters such as normals and curvatures and recover the exact interface geometry only in the limit of mesh refinement. In this paper, an explicit boundary tracking method is introduced which allows topological changes such as coalescence without requiring collision detection and intersection computations. The interface representation is used to generate signed algebraic level sets during analysis, and topological changes are translated into Boolean compositions on these level sets using R-functions. This allows easy evolution of the interface while retaining its geometric representation exact to its spline model. The developed procedure is used to study the evolution and coalescence of voids in a metal line carrying current. Since non-iterative, algebraic methods are used, the procedure is both stable and computationally efficient.

Keywords: Distance Fields, Algebraic Level Sets, Boolean Compositions, CAE, Isogeometric Analysis
DOI: https://doi.org/10.14733/cadaps.2020.1177-1192

1 INTRODUCTION

Moving boundaries refer to a large class of problems where the boundaries evolve with time, such as solidification, void formation, fracture or shape optimisation. Topological changes to geometry may arise naturally driven by the governing physics, or may be used as a means to design components with lower mass or higher

performance. For example, during nucleation and growth of a void due to high current density in a line (referred as electromigration) topological changes such as void coalescence and separation are common. If the evolving interface in such problems is represented explicitly e.g. using parametric splines, handling topological changes becomes challenging, requiring contact detection and computing surface-surface intersections. For example, if two voids are at the onset of coalescence, one needs to first detect when the associated closed geometries come in contact. As the voids coalesce, the merged geometries need to be described. This generally involves computing the surface-surface intersection of the two voids. Common strategies for contact detection and intersection computation include subdivision, marching, lattice evaluation and implicitisation [13]. Performing such operations at every time step becomes computationally expensive. Consequently, such phenomena are generally modeled using an implicit representations of the phase interface, most commonly using the phase-field or level set methods. In these methods, a state variable such as the phase field variable or the level set parameter with a corresponding evolution equation is introduced. The evolution of the phase interface is then described by the evolution of this state variable. While this implicit representation of phase boundaries naturally allows arbitrary topological changes, it comes at the cost of not having an explicit representation for the interface. This lack of explicit interface geometry is significant for phase evolution phenomena which depend on the curvature of, and the normal to the interface at a point. Additionally, the evolution equations either require stabilisation or are high order partial differential equations, resulting in prohibitive computational cost. In order to overcome the difficulty in the evolution of the interface as well as to retain its accuracy to its parametric spline geometric model, an explicit boundary tracking method that allows arbitrary topological changes is described in this paper.

In the present paper, the phase interface is explicitly described by a parametric spline representation, and its influence on the underlying domain is captured through an enrichment to the field approximation defined over the domain. The construction of behavioral approximations isoparametric with parametric spline geometric models was proposed early by the corresponding author among others [4, 12, 15, 18]. The use of such approximations for analysis is at present popularly referred as Isogeometric Analysis (IGA, [11]). The building of enriched approximations proposed by the corresponding author and co-workers [21] is referred as Enriched Isogeometric Analysis or EIGA. The influence of any enrichment, behavioral or otherwise, is generally expected to decrease with distance (see for instance heterogeneous material modeling using distance fields, [3]). Thus, behavioral enrichments require a measure of distance from the interface. Conventionally, such distance estimates from parametric geometries are obtained using the iterative Newton-Raphson technique [7, 14, 17]. However, numerical iterations are expensive and are often not sufficiently smooth for analysis purposes. A simpler approach to estimating the distance from a parametric geometry is to replace the geometry with a polytope approximation. Since distance from the planar segment can be easily computed, the distance from the geometry can be obtained easily as the least of such distances. The process can be handled through use of efficient data structures [10, 16]. However, the distance thus obtained is not smooth at the vertices and edges of the polytope approximation. This can be overcome by using R-functions to combine distance fields from individual segments into a single, smooth distance field for the parametric geometry [2]. Nevertheless, these methods lose the geometric exactness of the phase interface and are accurate only in the limit of refinement.

In this paper, signed algebraic level sets of the interface are generated using implicitisation of its parametric representation employing the resultant theory [19, 23]. These level sets act as a smooth surrogate for distance and can hence be used to model the weakening influence of the enrichment. They are exact in the neighbourhood of the curve or surface and thus preserve geometric accuracy. Since they are generated through a non-iterative algebraic process, they are also numerically efficient. Furthermore, for closed geometries, these algebraic level sets are signed, in that they classify points as lying inside or outside the closed geometry [24]. This helps determine the phase at a given point in space during analysis. Since analysis is based on algebraic level sets instead of the explicit parametric representation of the interface, topological changes in the phases can be modeled through algebraic Boolean operations on these level sets using R-functions [20, 24]. The usage of R-functions ensures that the resultant field retains the smoothness and geometric accuracy of the

individual fields. Implicit surface representation has been used for modeling in haptics [9], quadric surface fitting [1] and in filling holes in polygonal meshes [25]. Prior work using algebraic Boolean operations using R-functions for analysis also exist in the literature. In [6, 26], Boolean operations were used during topology optimization to combine free-form geometries with embedded regular-shaped primitives. In general, algebraic Boolean compositions of complex free form parametric geometries do not appear to exist except for that in [24]; they carried out Boolean operations on algebraic level sets constructed on complex parametric CAD geometry. These were then used for static thermal and mechanical analysis.

In the present paper, Boolean compositions on algebraic level sets are used to study void coalescence in a metal line subjected to high current density. When very thin lines carry current in Integrated Circuits (ICs), large electric fields develop. Under such electric fields, electrons carry sufficient momentum to impart large forces to the metal ions in the line, thereby displacing them. This leads to formation of voids near the cathode and accumulation of material (called 'hillocks') near the anode. This phenomenon is called electromigration. As current continues to pass through the line, the developed voids evolve and grow until an open circuit failure eventually results. During evolution, these voids can undergo drastic topological changes such as splitting or coalescence with other voids, making this problem appropriate for application of the developed procedure. Thus, in this paper, this evolution of voids under an electric field is studied, and coalescence of multiple interacting voids is used to demonstrate the ability to handle topological changes.

This paper is organized as follows. First, implicitisation of parametric surfaces using the Dixon resultant is discussed in § 2. The resultant is used in § 3 to generate signed algebraic level sets. These level sets act as a surrogate of distance for parametric geometries since they increase monotonically with distance. The Enriched Isogeometric Analysis (EIGA) procedure for electromigration is described in § 4, which uses a distance-based weighted blending of a continuous approximation, and an enrichment representing the influence of a void. The signed algebraic level sets generated in § 3 are used as a measure of distance for this weighted blending. This approach however does not handle topological changes such as void coalescence when there are multiple, interacting voids. A discussion on the handling of such topological changes using Boolean compositions of algebraic level sets is provided in § 5. The paper concludes with examples of electromigration driven void evolution with multiple interacting voids.

2 IMPLICITIZATION USING THE DIXON RESULTANT

Curves and surfaces can be expressed with an implicit or a parametric representation. Most CAD systems use the parametric Non-Uniform Rational B-Splines (NURBS) representation, which provides a more general as well as intuitive control of the geometry for users. On the other hand, the implicit representation of a surface allows natural generation of level sets that increase monotonically with distance and hence are convenient for analysis. For instance, for a unit sphere centered at the origin, the implicit function $f(\mathbf{x}) = x^2 + y^2 + z^2 - 1$ generates level sets that are zero on the surface of the sphere but increase monotonically in magnitude as we move away from it. It is hence desirable to obtain the equivalent implicit representation for a given parametric curve or surface for use in analysis as discussed in § 1. One possible approach to achieving this is through the Resultant theory.

Resultants are polynomial expressions on the coefficients of a given system of polynomial equations. A given system of equations has a common solution only if its resultant vanishes. For example, for a linear system $\mathbf{Ax} = 0$, the determinant of the coefficient matrix, $|\mathbf{A}|$, can serve as a resultant; it depends only on the coefficients of the system, and the system has a non-trivial solution only if the determinant vanishes. One commonly used resultant is the Dixon resultant [8]. This is an n-dimensional generalisation of the Cayley-Bezout resultant [5] developed for a system of two uni-variate polynomial equations. In this paper, the Dixon resultant is used to implicitise parametric geometries by treating the parametric representation as a polynomial system of equations [19]. A procedure to compute the Dixon resultant shall be discussed presently. While the procedure described is for three-dimensional surfaces, it can be readily adapted for planar curves.

Rational parametric representations such as Bézier and NURBS have the general form,

$$x(u,v) = \frac{X(u,v)}{W(u,v)}, y(u,v) = \frac{Y(u,v)}{W(u,v)}, z(u,v) = \frac{Z(u,v)}{W(u,v)} \tag{1}$$

where, X, Y, Z, W are functions in the parameters (u, v), with degree m in u and n in v. Such representations can be converted into a polynomial system of equations,

$$\begin{aligned} xW(u,v) - X(u,v) &= 0 \\ yW(u,v) - Y(u,v) &= 0 \\ zW(u,v) - Z(u,v) &= 0 \end{aligned} \tag{2}$$

The Dixon resultant is now developed for this polynomial system. Define, for some real constants α, β,

$$\delta(\mathbf{x}) = \frac{1}{(u-\alpha)(v-\beta)} \begin{vmatrix} xW(u,v) - X(u,v) & yW(u,v) - Y(u,v) & zW(u,v) - Z(u,v) \\ xW(u,\beta) - X(u,\beta) & yW(u,\beta) - Y(u,\beta) & zW(u,\beta) - Z(u,\beta) \\ xW(\alpha,\beta) - X(\alpha,\beta) & yW(\alpha,\beta) - Y(\alpha,\beta) & zW(\alpha,\beta) - Z(\alpha,\beta) \end{vmatrix}$$

Since the determinant is zero whenever $u = \alpha$ or $v = \beta$, $(u - \alpha)$ and $(v - \beta)$ are factors of the determinant and have hence been factored out. From Eq. (2), for points on the surface, the first-row entries are zero, and the determinant is zero irrespective of α, β. Hence all points on the surface satisfy,

$$\delta(\mathbf{x}) = 0 \qquad \forall\ \alpha, \beta \in \mathbb{R} \tag{3}$$

Now, the quantity δ depends on α, β and u, v, and can be expanded to separate these factors as,

$$\delta(\mathbf{x}) = \begin{bmatrix} 1 & \alpha & \alpha^2 & \cdots & \alpha^{m-1}\beta^{2n-1} \end{bmatrix} [\mathbf{M_D}(\mathbf{x})] \begin{bmatrix} 1 & u & u^2 & \ldots & u^{2m-1}v^{n-1} \end{bmatrix}^{\mathrm{T}} = [\boldsymbol{\alpha}][\mathbf{M_D}(\mathbf{x})][\mathbf{u}] \tag{4}$$

where, $\boldsymbol{\alpha}$ and $\mathbf{u}$ denote the corresponding vectors on either side of $[\mathbf{M_D}]$ in Eq. (4). For the quantity $\delta(\mathbf{x})$ to vanish for all α, β, we require,

$$[\mathbf{M_D}(\mathbf{x})][\mathbf{u}] = 0 \tag{5}$$

$$\Rightarrow |\mathbf{M_D}(\mathbf{x})| = 0 \tag{6}$$

This forms a necessary condition for a point to lie on the parametric surface and can act as its implicit equation. The $2mn \times 2mn$ determinant in Eq. (6) is the Dixon resultant. The corresponding matrix is linear in x, y, z and independent of u, v, and can be expressed as [8],

$$\mathbf{M_D}(\mathbf{x}) = \mathbf{M_x}x + \mathbf{M_y}y + \mathbf{M_z}z + \mathbf{M_w} \tag{7}$$

where each of the coefficients are constants and independent of u, v or $\mathbf{x}$. An algorithm to build the Dixon matrix $\mathbf{M_D}$ from a given parametric representation is provided in [19].

3 GENERATING SIGNED ALGEBRAIC LEVEL SETS

The Dixon resultant derived in Eq. (6) allows the generation of the level sets [23],

$$\Gamma(\mathbf{x}) = |\mathbf{M_D}(\mathbf{x})| \tag{8}$$

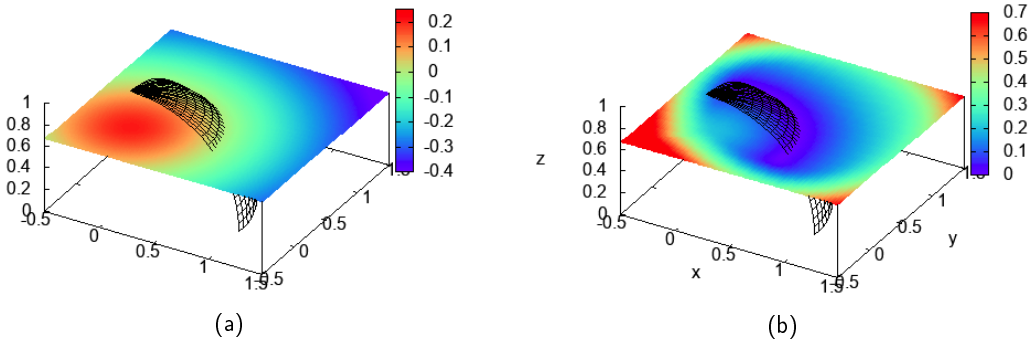

Figure 1: Algebraic level sets for an octant of a sphere generated from (a) Dixon resultant and (b) after the trimming operation.

The generated level sets for an octant of a sphere are shown in Fig. 1a. It can be seen that while the parametric surface is restricted to just an octant, the resultant generates level sets over the entire parametric range, i.e., for the entire sphere. This is because the implicit equation for an octant of a sphere is the same as that for the whole sphere. Hence, as we move away from the surface in the radially inward direction, the level sets are not monotonic functions of distance. It is hence necessary that the implicitisation is restricted to the required parametric domain. This can be achieved using a trimming procedure based on R-functions [2, 20]. The convex hull of the parametric surface, defined by the field $\Phi(\mathbf{x}) \geq 0$, is used as the trimming region. The trimming is carried out in two steps: normalization of the level sets generated from the resultant, and composition with the trimming region using R-functions. Both steps shall be discussed in brief presently.

3.1 Normalization of the Level Sets

The algebraic level sets generated from Eq. (8) do not inherently satisfy $\|\nabla\Gamma\| = 1$ on the boundary or surface of the geometry. Thus, the level sets could grow at different rates in the neighborhood of the curve or surface in comparison with the hull distance field. Consequently, in order to compose these level sets with the hull distance field, they first have to be normalized.

Consider a point $\mathbf{x}$, a distance d away from the geometry. Let $\mathbf{x}_f$ be the projection of this point on to the curve or surface. The Taylor expansion of the resultant about the point $\mathbf{x}$ gives,

$$\Gamma(\mathbf{x}_f) = \Gamma(\mathbf{x}) - \nabla\Gamma(\mathbf{x}) \cdot d\mathbf{n} + \frac{d^2}{2}\mathbf{n} \cdot \nabla\nabla\Gamma(\mathbf{x}) \cdot \mathbf{n} + \dots \tag{9}$$

where, $\mathbf{n}$ is the unit normal to the curve or surface at $\mathbf{x}_f$. Since $\mathbf{x}_f$ lies on the geometry, $\Gamma(\mathbf{x}_f) = 0$. Ignoring higher order terms, we have the first order distance estimate,

$$f(\mathbf{x}) = d = \frac{\Gamma(\mathbf{x})}{\|\nabla\Gamma(\mathbf{x})\|} \tag{10}$$

This distance measure automatically satisfies $\|\nabla f(\mathbf{x})\| = 1$ on the boundary (where $\Gamma(\mathbf{x}) = 0$), and can hence generate normalized algebraic level sets. The gradient of the resultant can be obtained using Jacobi's formula in Eqs. (7) and (8).

3.2 Trimming Operation Using R-Functions

The trimmed algebraic level set, $g(\mathbf{x})$, is now given by the R-function [22],

$$g(\mathbf{x}) = \sqrt{f^2 + \frac{\left(|\Phi| - \Phi\right)^2}{4}} = \begin{cases} |f(\mathbf{x})| & \Phi(\mathbf{x}) \geq 0 \\ \sqrt{f^2 + \Phi^2} & \Phi(\mathbf{x}) < 0 \end{cases} \tag{11}$$

Within the trimming region, the original implicitisation is recovered, while outside the region a composite field is obtained. This ensures that the subsequent level sets are smooth everywhere. The distance field Φ for the convex hull can be computed as a Boolean union of distance fields of its individual faces (edges in 2D). The procedure to obtain the Boolean union is described in § 5 as the R-disjunction operation. Trimmed level sets generated for the sphere octant are shown in Fig. 1b; it can be seen that the level sets are globally monotonically increasing.

For parametric splines such as NURBS, Eq. (1), and therefore the resultant, change with each knot span. Such splines are first decomposed into their Bézier segments, each segment corresponding to a single knot span. Trimmed normalized algebraic level sets are then obtained for each Bézier segment through the procedure described in this section. These level sets are then composed using a R-disjunction operation [20] to obtain smooth algebraic level sets for the whole parametric spline. An illustration is provided in Fig. 2, where algebraic level sets for a NURBS curve are generated from trimmed level sets of its two constituent Bézier segments. The resulting level sets are also smooth and trimmed. Information on the R-disjunction operation is provided in § 5.

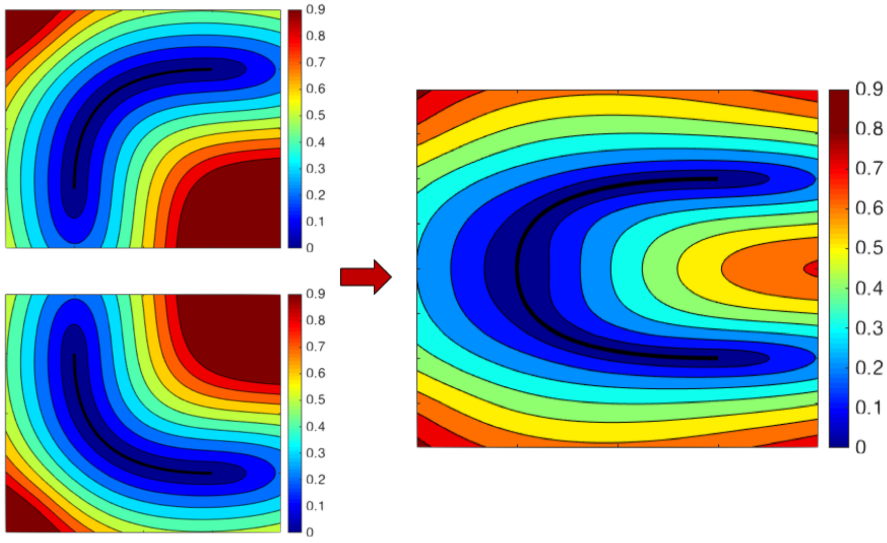

Figure 2: Algebraic level sets for a spline obtained from R-function based composition of level sets of individual Bézier segments.

3.3 Ascribing Sign to Algebraic Level Sets

Closed geometries divide space into inside and outside regions. This allows one to define signed algebraic level sets. As a convention, in this paper, distances of points in the inside region are assumed positive and those

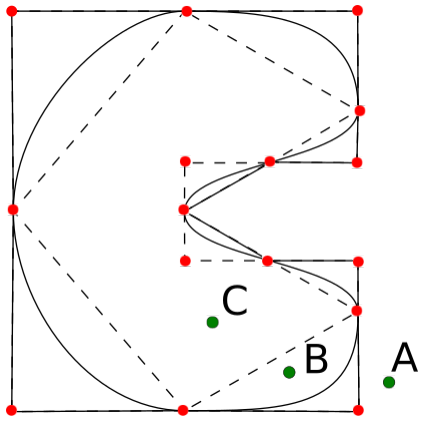

Figure 3: Schematic describing the sign assignment process with three illustrative points. The convex hulls for constituent Bézier segments are shown. The edges of the hulls contributing to the bounding box are shown solid, while the rest are dashed.

outside, negative. Signed algebraic level sets can be used to resolve point containment queries, required in multi-body contact and interference detection. In the context of analysis, point containment queries determine the phase, and hence the material properties, at a particular point in space. These queries can be handled on a point-by-point basis using a bounding box procedure described in [24] and outlined here. The given closed spline geometry is decomposed into its constituent Bézier segments. The convex hulls of the individual segments are then used to form a close-fitted bounding polygon for the geometry, called its bounding box. For each Bézier component, the sign of the Dixon resultant $\Gamma(\mathbf{x})$ is set such that the resultant is negative for control points that lie on the bounding polygon (and hence outside the geometry). This ensures that within the convex hull of any Bézier component, points outside the closed geometry have negative resultant values and those inside, positive. This is a one-time process for a given geometry.

During sign determination, the point of interest is first classified with respect to the bounding box. If the point is outside the bounding box, then it is also outside the given geometry and its level set can be taken to be negative. Query points that lie inside the bounding box are then classified with respect to the convex hulls of the Bézier components. If the point lies inside any of the hulls, then the sign of the algebraic level set is the same as the sign of the Dixon resultant of the corresponding Bézier component, evaluated at that point. If the query point does not lie inside any of the individual convex hulls, but lies inside the bounding box, then it lies inside the closed geometry and its level set can be taken to be positive. This is described in the schematic shown in Fig. 3. Three points, A, B and C are chosen as shown. Point A lies outside the bounding box and hence has a negative level set. Point B lies inside the convex hull of a segment; its sign is assigned based on the sign of the Dixon resultant of the segment at B (here positive). Point C lies inside the bounding box, but not inside any of the convex hulls. From the construction of the bounding box, this implies that C lies inside the closed geometry and thus has a positive level set. An example of signed algebraic level sets for a sphere is given in Fig. 4.

4 CURRENT THROUGH A LINE WITH A VOID

As an application, the electrostatic problem of a current carrying metal line with a void is considered. This is of relevance in studying void growth due to electromigration, which is a failure concern in the semiconductor industry. A formal description of the electromigration problem follows (see Fig. 5a for reference). A rectangular domain Ω, containing an arbitrarily shaped void is considered. To allow irregular shapes, voids are represented

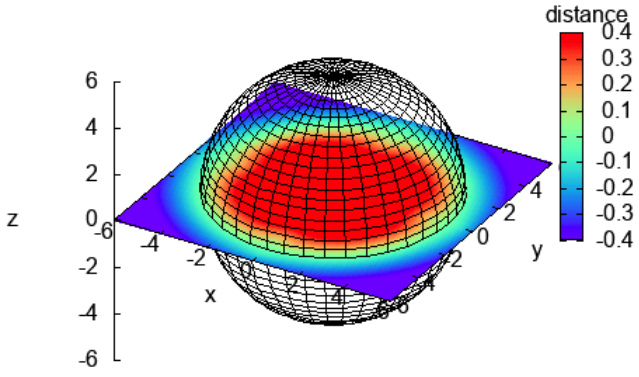

Figure 4: Signed algebraic level sets for a sphere generated using the bounding box procedure. Regions inside the sphere have positive level sets and those outside, negative.

using unclamped NURBS curves. The usage of unclamped curves ensures C^1 continuity of both geometry and electric potential approximation. The system is governed by the Laplace equation on the electric potential ϕ,

$$\Delta\phi = 0 \quad \text{in } \Omega \tag{12}$$

Dirichlet boundary conditions are applied at the top and bottom surfaces, and the walls are assumed to not allow electric flux to flow through them. Additionally, there is no flux entering or exiting the surface of a void Γ_e,

$$\frac{\partial\phi}{\partial n} = 0 \quad \text{on } \Gamma_e \tag{13}$$

Here, an enriched isogeometric approach is used [21], where the potential is expressed as a weighted blending of a continuous approximation ϕ_c, and an enrichment ϕ_e representing the influence of the void,

$$\phi(\mathbf{x}) = (1 - w(\mathbf{x}))\,\phi_c(\mathbf{x}) + w(\mathbf{x})\phi_e(\mathcal{P}(\mathbf{x})) \tag{14}$$

Here, $\mathcal{P}(\mathbf{x})$ is the projection of $\mathbf{x}$ on to the void interface (see Fig. 5a). Thus, the potential solution ϕ_c at $\mathbf{x}$ is blended with the interface solution ϕ_e at the projection of $\mathbf{x}$ on the void interface. The weight function $w(\mathbf{x})$ is defined such that it is unity on the void boundary and falls monotonically to zero with distance away from the void,

$$w(\mathbf{x}) = \exp\left(-\left(\frac{d(\mathbf{x})}{d_0}\right)^2\right) \tag{15}$$

where, d_0 is a scaling parameter for the distance field $d(\mathbf{x})$. This ensures that the solution near the void interface is dominated by the interface solution ϕ_e, while the continuous solution dictates behavior at points far away from the void. Since the void is represented as a NURBS curve, the signed algebraic level sets described in this work can be used as the distance measure. This form of the electric potential automatically satisfies the void boundary condition Eq. (13). The system is solved using isogeometric analysis for an elliptical void, and the resulting potential solution is shown in Fig. 5b.

The obtained results can be interpreted as follows. For a system with no voids, the analytical solution at a point $\mathbf{x} \equiv (x, y)$ is given by,

$$\phi(\mathbf{x}) = \frac{y}{h} \tag{16}$$

where, h is the height of the metal line. The potential solution varies linearly from the bottom surface to the top. This satisfies both the governing Laplace equation, as well as the Dirichlet and wall boundary conditions.

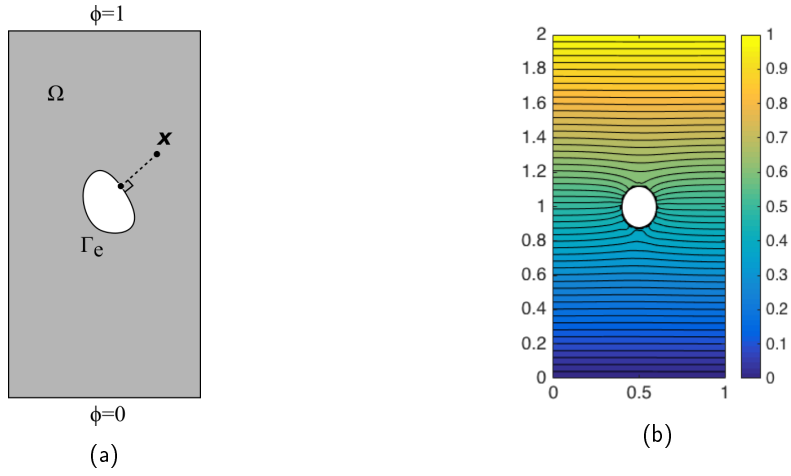

Figure 5: (a) Schematic of the electromigration problem for a rectangular domain. A sample point and its projection on to the void interface are illustrated. (b) Contours of the electric potential solution obtained for a system with a single void.

Such a solution is characterized by straight, horizontal contour lines. As can be seen in Fig. 5b, far away from the void, the potential contour lines are unaffected and remain straight and horizontal. However in the neighbourhood of the void, the contours are distorted in order to satisfy Eq. (13). The use of an explicit interface representation along with the assumed form for the potential approximation in Eq. (14) has allowed imposing the void interface conditions exactly.

5 BOOLEAN OPERATIONS FOR MULTIPLE VOID SYSTEMS

Complications arise in modeling electromigration problems when multiple interacting voids are present. Voids can split or coalesce with one another, and this poses a challenge for explicit interface representations. Such representations usually require detection of contact between coalescing voids and computation of intersections of the void boundaries. These are challenging problems with arbitrarily shaped voids. In this work, this problem is circumvented by using Boolean operations on the algebraic level sets. The algebraic Boolean union of the level sets of individual void interfaces is used for analysis. As voids coalesce, the union operation automatically generates algebraic level sets for the coalesced void. Since the analysis procedure depends only on algebraic level sets, this Boolean union of the level sets suffices and interacting voids can be easily accommodated without requiring collision detection and intersection computations. The union operation is carried out using the R-disjunction operation [20]. If $g_1(\mathbf{x})$ and $g_2(\mathbf{x})$ are the signed algebraic level sets of two coalescing voids, then the union of these level sets is given by,

$$g(\mathbf{x}) = g_1 \vee g_2 = g_1(\mathbf{x}) + g_2(\mathbf{x}) + \sqrt{g_1^2 + g_2^2} \tag{17}$$

By the nature of the R-disjunction, the resultant signed level set is positive when either level set is positive; this ensures that the region inside a coalesced void is positive. This is depicted in Fig. 6 for a system with two voids. As can be seen from the figure, the union operation ensures positive level sets inside either void, and thus automatically generates algebraic level sets for a coalesced void. The usage of R-disjunction ensures that the composed algebraic level sets are smooth, allowing analysis. A system with two elliptical voids was studied. The solution for the electric potential for the system with and without coalescence of the voids is shown

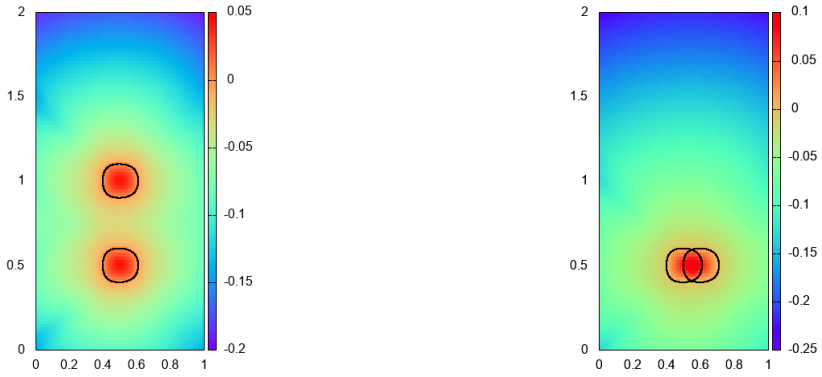

(a) (b)

Figure 6: Algebraic level sets for a system with two interacting voids (a) without coalescence (b) with coalescence. The level sets are generated through a Boolean union operation on individual level sets in both cases.

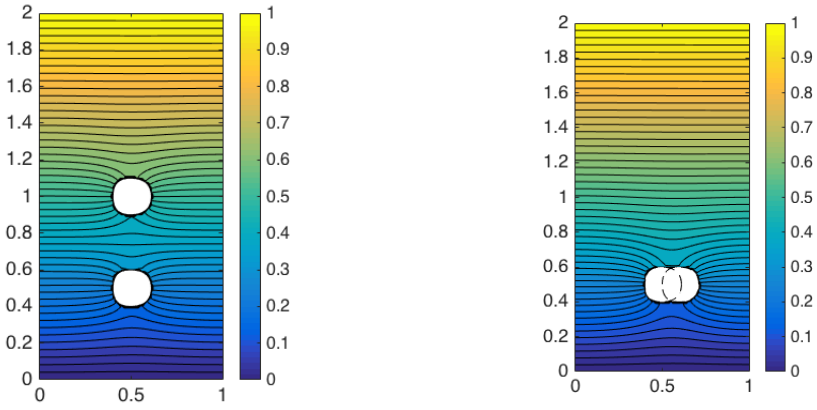

(a) (b)

Figure 7: Contours of the electric potential solution for a system with two interacting voids (a) without coalescence (b) with coalescence.

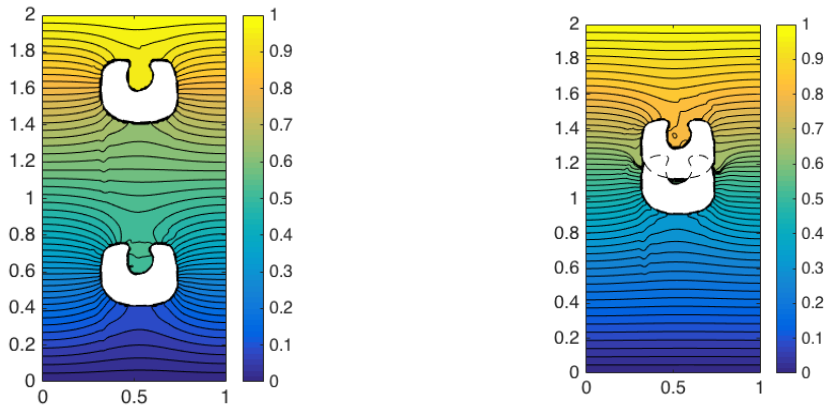

(a) (b)

Figure 8: Contours of the electric potential solution for a system with two bean-shaped interacting voids (a) without coalescence (b) with coalescence.

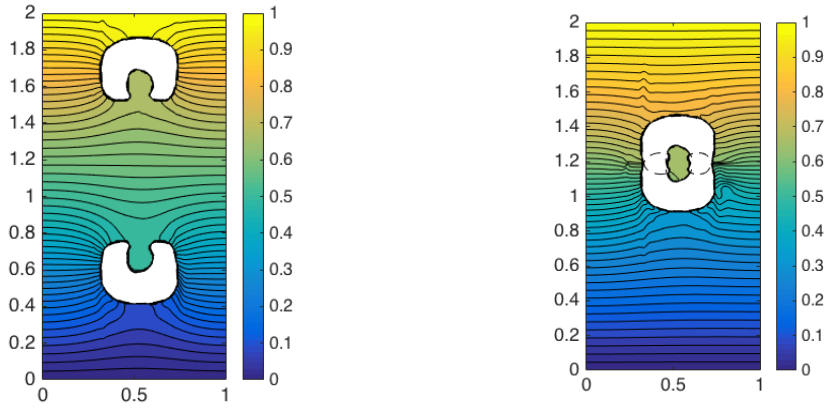

(a) (b)

Figure 9: Contours of the electric potential solution for a system with two bean-shaped interacting voids (a) without coalescence (b) with coalescence.

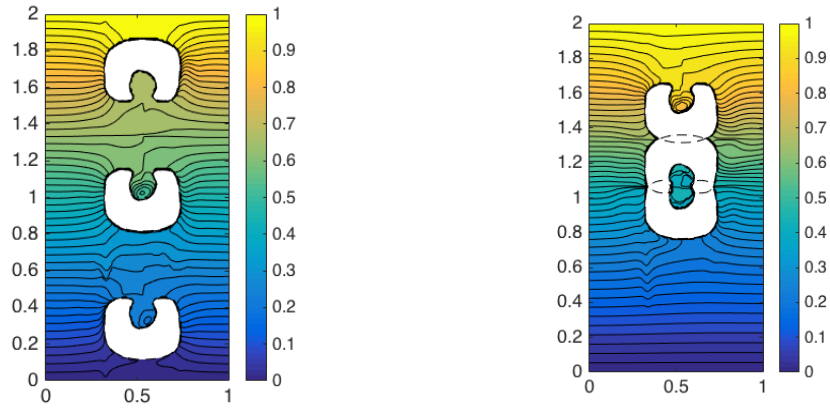

(a) (b)

Figure 10: Contours of the electric potential solution for a system with three bean-shaped interacting voids (a) without coalescence (b) with coalescence.

in Fig. 7. The proposed method was also applied to systems with bean-shaped voids defined as unclamped NURBS curves. The solution for the electric potential for such systems with and without coalescence is shown in Figs. 8 to 10. For these examples, an explicit interface representation would have to detect multiple complex surface-surface intersections and handle them appropriately. These difficulties are easily overcome using the proposed approach. Three-dimensional examples of a system with spherical voids is given in Figs. 11 and 12. The computation times for all the above cases is tabulated in Tab. 1. As can be seen from the table, there is no significant overhead on handling systems with coalescent voids. However, simulations with multiple voids took significantly more computational time than systems with a single void. Thus the proposed approach allows one to use an explicit interface representation, retaining exact geometric information, while also providing the ability to model topological changes such as coalescence at low computational costs.

6 CONCLUSIONS

The Dixon resultant was used to generate signed algebraic level sets for parametric geometries. The magnitude of these level sets provided a measure of distance from the geometry, while the sign enabled classifying points as lying inside or outside a given closed geometry. An enriched isogeometric analysis method for a current carrying metal line with a void was discussed. The void was modeled as an enrichment whose influence weakened with distance. Due to the explicit interface representation and the form of the potential approximation, the void interface conditions are imposed exactly. It was shown that topological changes such as coalescence could be handled through Boolean operations on the algebraic level sets, carried out using R-functions. This allowed handling topological changes without having to resort to overlap detection and intersection computations. This was demonstrated on 2D and 3D systems with coalescing voids.

A study of the computational efficiency shows that while the computational time increased with increase in number of voids, there was no significant overhead for handling topological changes such as coalescence. Systems with coalescent voids took slightly less time than those without, which is in stark contrast to other explicit representation methods. The developed procedure thus provides the benefits of using explicit interface representations without requiring intersection computation to model topological changes.

Electromigration is also known to cause voids to split. The splitting of a void can be geometrically

Electromigration System	Number of Degrees of Freedom	Time Without Coalescence (in s)	Time With Coalescence (in s)
One 2D elliptical void (Fig. 5)	237	0.12	N/A
Two 2D elliptical voids (Fig. 7)	243	0.27	0.20
Two 2D bean-shaped voids (Fig. 8)	259	0.99	0.73
Two 2D bean-shaped voids (Fig. 9)	259	1.01	0.95
Three 2D bean-shaped voids (Fig. 10)	273	2.15	1.61
One 3D spherical void (Fig. 11)	4896	10.99	N/A
Two 3D spherical voids (Fig. 12)	4941	30.41	26.34

Table 1: Computation times for electromigration simulations of the different systems considered. The systems are referred by the index of the corresponding figure. There is no significant overhead on handling systems with coalescent voids.

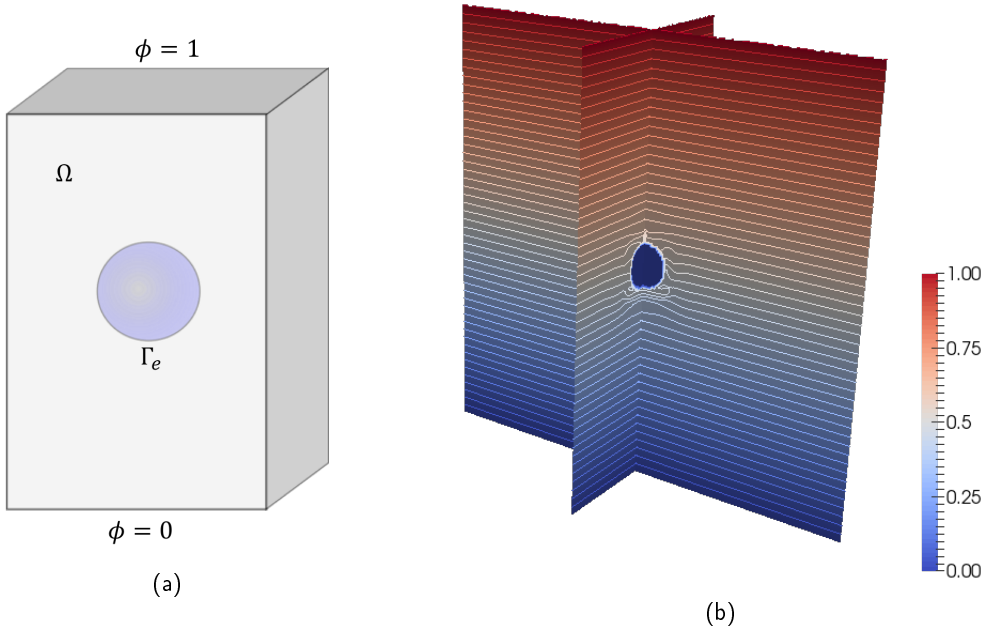

Figure 11: (a) Schematic of the 3D electromigration problem with a single spherical void. (b) Contours of the electric potential solution obtained on the mid-section planes.

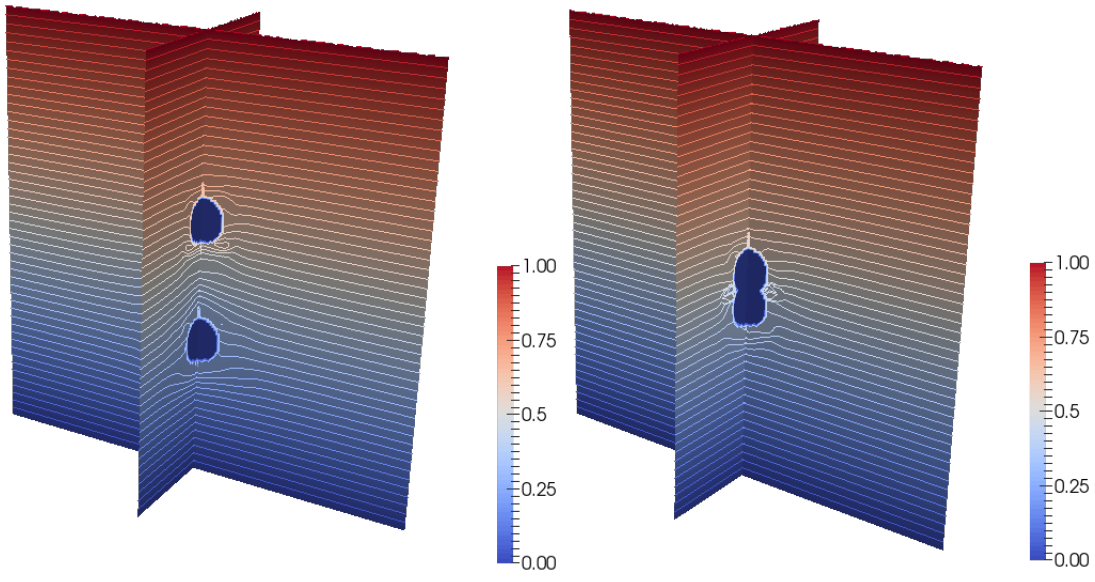

Figure 12: (a) Schematic of the 3D electromigration problem with coalescent spherical voids. (b) Contours of the electric potential solution obtained on the mid-section planes.

characterized as a self-intersection of the void surface. Since the detection of self-intersections is not a trivial operation, further work is required to handle systems with void splitting.

ORCID

Pavan Kumar Vaitheeswaran, http://orcid.org/0000-0002-0429-534X
Ganesh Subbarayan, http://orcid.org/0000-0003-0462-1130

REFERENCES

[1] Andrews, J.; Séquin, C.H.: Type-constrained direct fitting of quadric surfaces. Computer-Aided Design and Applications, 11(1), 107–119, 2014. http://doi.org/10.1080/16864360.2013.834155.

[2] Biswas, A.; Shapiro, V.: Approximate distance fields with non-vanishing gradients. Graphical Models, 66, 133–159, 2004. http://doi.org/10.1016/j.gmod.2004.01.003.

[3] Biswas, A.; Shapiro, V.; Tsukanov, I.: Heterogeneous material modeling with distance fields. Computer Aided Geometric Design, 21, 215–242, 2004. http://doi.org/10.1016/j.cagd.2003.08.002.

[4] Cassale, M.: Integration of Geometric Analysis and Structural Analysis using Trimmed Patches. Ph.D. thesis, University of California, Irvine, 1989.

[5] Cayley, A.: On the theory of elimination. Cambridge and Dublin Mathematical Journal, 3, 116–120, 1848.

[6] Chen, J.; Shapiro, V.; Suresh, K.; Tsukanov, I.: Shape optimization with topological changes and parametric control. International Journal for Numerical Methods in Engineering, 71(3), 313–346, 2007. http://doi.org/10.1002/nme.1943.

[7] Chen, X.D.; Yong, J.H.; Wang, G.; Paul, J.C.; Xu, G.: Computing the minimum distance between a point and a NURBS curve. Computer-Aided Design, 40(10-11), 1051–1054, 2008. http://doi.org/10.1016/j.cad.2008.06.008.

[8] Dixon, A.: On a form of the eliminant of two quantics. Proceedings of the London Mathematical Society, 2, 468–478, 1908. http://doi.org/10.1112/plms/s2-6.1.468.

[9] Gao, Z.; Gibson, I.: Haptic b-spline surface sculpting with a shaped tool of implicit surface. Computer-Aided Design and Applications, 2(1-4), 263–272, 2005. http://doi.org/10.1080/16864360.2005.10738374.

[10] Guezlec, A.: "Meshsweeper": dynamic point-to-polygonal mesh distance and applications. IEEE Transactions on Visualization and Computer Graphics, 7(1), 47–61, 2001. http://doi.org/10.1109/2945.910820.

[11] Hughes, T.; Cottrell, J.; Bazilevs, Y.: Isogeometric analysis: CAD, finite elements, NURBS, exact geometry and mesh refinement. Computer Methods in Applied Mechanics and Engineering, 194(39-41), 4135–4195, 2005. http://doi.org/10.1016/j.cma.2004.10.008.

[12] Kagan, P.; Fischer, A.: Integrated mechanically based CAE systems using B-spline based finite elements. Computer Aided Design, 32, 2000. http://doi.org/10.1016/S0010-4485(00)00041-5.

[13] Krishnan, S.; Manocha, D.: An efficient surface intersection algorithm based on lower-dimensional formulation. ACM Transactions on Graphics, 16(1), 74–106, 1997. http://doi.org/10.1145/237748.237751.

[14] Ma, Y.L.; Hewitt, W.T.: Point inversion and projection for NURBS curve and surface: control polygon approach. Computer Aided Geometric Design, 20(2), 79–99, 2003. http://doi.org/10.1016/S0167-8396(03)00021-9.

[15] Natekar, D.; Zhang, X.; Subbarayan, G.: Constructive solid analysis: a hierarchical, geometry-based meshless analysis procedure for integrated design and analysis. Computer-Aided Design, 36(5), 473–486, 2004. http://doi.org/10.1016/S0010-4485(03)00129-5.

[16] Payne, B.A.; Toga, A.W.: Distance field manipulation of surface models. IEEE Computer Graphics and Applications, (1), 65–71, 1992. http://doi.org/10.1109/38.135885.

[17] Piegl, L.; Tiller, W.: The NURBS Book. Springer Science & Business Media, 2012.

[18] Renken, F.; Subbarayan, G.: NURBS based solution to inverse boundary problems in droplet shape prediction. Computer Methods in Applied Mechanics and Engineering, 190, 1391–1406, 2000. http://doi.org/10.1016/S0045-7825(00)00168-7.

[19] Sederberg, T.W.: Implicit and Parametric Curves and Surfaces for Computer Aided Geometric Design. Ph.D. thesis, Purdue University, 1983.

[20] Shapiro, V.: Theory of R-functions and Applications: A Primer. Technical Report, Cornell University, 1991.

[21] Tambat, A.; Subbarayan, G.: Isogeometric enriched field approximations. Computer Methods in Applied Mechanics and Engineering, 245, 1–21, 2012. http://doi.org/10.1016/j.cma.2012.06.006.

[22] Tsukanov, I.; Shapiro, V.: Implicit functions with guaranteed differential properties. In Proceedings of the Fifth ACM Symposium on Solid Modeling and Applications, 258–269, 1999. http://doi.org/10.1145/304012.304038.

[23] Upreti, K.; Song, T.; Tambat, A.; Subbarayan, G.: Algebraic distance estimation for enriched isogeometric analysis. Computer Methods in Applied Mechanics and Engineering, 280, 28–56, 2014. http://doi.org/10.1016/j.cma.2014.07.012.

[24] Upreti, K.; Subbarayan, G.: Signed algebraic level sets on NURBS surfaces and implicit Boolean

compositions for isogeometric CAD-CAE integration. Computer-Aided Design, 82, 112–126, 2017. http://doi.org/10.1016/j.cad.2016.09.006.

[25] Wu, X.J.; Wang, M.Y.; Han, B.: An automatic hole-filling algorithm for polygon meshes. Computer-Aided Design and Applications, 5(6), 889–899, 2008. http://doi.org/10.3722/cadaps.2008.889-899.

[26] Xia, L.; Zhu, J.; Zhang, W.; Breitkopf, P.: An implicit model for the integrated optimization of component layout and structure topology. Computer Methods in Applied Mechanics and Engineering, 257, 87–102, 2013. http://doi.org/10.1016/j.cma.2013.01.008.